THE ASTROPHYSICAL JOURNAL, 264:282–295, 1983 January 1

A ONE-ZONE MODEL FOR SHELL FLASHES ON ACCRETING COMPACT STARS

BOHDAN PACZYŃSKI[1,2]
Theoretical Astrophysics, California Institute of Technology
Received 1982 March 19; accepted 1982 June 30

ABSTRACT

A one-zone model is developed for analysis of properties of nuclear shell flashes on accreting degenerate dwarfs and neutron stars. The model provides a description of a steady-state nuclear burning and a linear stability analysis with a small number of algebraic equations. Time evolution of the accreted layer is described with two first order ordinary differential equations: one for the heat balance, the second for the mass balance. A very small computing power is required for the analysis. This makes the model attractive for pilot studies, for a simple analysis of many properties of compact stars accreting nuclear fuel, and for teaching purposes.

When the accretion rate is either very low or very high, then column density increases with the accretion rate and the models with a steady state nuclear burning are stable. For intermediate rates, the surface mass density decreases with increasing accretion rate and the models are thermally unstable. Near the transition from stability to instability the eigenvalues of the problem are always complex. The models are stable for any value of the accretion rate when either the heat flux from the core exceeds some critical value, or the accreted matter is rich in hydrogen but has no metals, so that nuclear burning may proceed through the proton-proton chain only.

Large-amplitude shell flashes develop for all unstable models provided that heat flux from the core is below certain value. The time interval between the flashes decreases with increasing surface gravity, accretion rate and heat flux from the core. The shortest periods for accreting degenerate dwarfs are just 1 month for hydrogen-rich matter and 1 year for helium-rich matter. The shortest interflash period for a neutron star accreting helium is only 10 s. The values of these periods may be incorrect by a factor of 2 or so, because of simplifications inherent in the one-zone model.

Subject headings: instabilities — stars: accretion — stars: neutron — stars: white dwarfs — X-rays: bursts

I. INTRODUCTION

Accretion of hydrogen- or helium-rich matter onto degenerate dwarfs or neutron stars may give rise to stable or unstable nuclear burning. Hydrogen ignition on accreting white dwarfs is believed to be responsible for explosions of classical novae (cf. Gallagher and Starrfield 1978 and references therein). Accretion of hydrogen onto white dwarfs may also be relevant for symbiotic stars (Paczyński and Rudak 1980). Helium shell flashes on accreting neutron stars may give rise to X-ray bursts (cf. Lewin and Joss 1981; Joss 1981; and references therein). It is believed that if the accretion rate is constant, then the shell flashes are recurrent, but only a few model computations were carried through more than one flash cycle (e.g., Paczyński and Żytkow 1978; Sion, Acierno, and Tomczyk 1979). Evolutionary computations (e.g., Paczyński and Żytkow 1978) and linear stability analysis (e.g., Sienkiewicz 1980) indicate that nuclear burning becomes stable when the accretion rate exceeds some critical value.

A number of attempts were made to understand qualitatively the nature of nuclear shell flashes and to gain some insight without following stellar evolution in all details with a large and time-consuming computer code. Recently, some semianalytical studies have been published or are in press (Paczyński 1980; Barranco, Buchler, and Livio 1980; Ergma and Tutukov 1980; Sugimoto and Miyaji 1981; Fujimoto, Hanawa, and Miyaji 1981; Papaloizou, Pringle, and MacDonald 1982; Fujimoto 1982). The aim of this paper is to present another semianalytical one-zone model for nuclear burning on accreting compact stars. I believe this model is simpler than the others, while it retains many of the essential features of full-scale stellar models. In particular, it permits construction of models with a steady-state nuclear burning, a linear stability analysis, nonlinear flash calculations, and reasonably good evaluation of the interflash period. The first two tasks may be easily accomplished on a pocket programmable calculator, while the latter two may be achieved on a desk-top computer. Description of the model with some examples of the results are given in the next chapter. A complete presentation of the results is given in the subsequent sections.

[1] Sherman Fairchild Distinguished Scholar at the California Institute of Technology.

[2] On leave from N. Copernicus Astronomical Center, Polish Academy of Sciences, Warsaw.

II. DESCRIPTION OF THE MODEL

Full-scale evolutionary computations of a number of shell flash cycles made by Paczyński and Żytkow (1978) provided many details of the interior structure and time variations of accreting degenerate dwarfs. It turned out that throughout most of the flash cycle all physical quantities varied monotonically in space: temperature, density, and pressure decreased with radius, while the hydrogen content and heat flux increased with radius. Also, a bulk of hydrogen-rich matter was close to the nuclear burning shell. The degenerate interior did not change much throughout the flash cycles. Therefore, it is reasonable to describe the whole hydrogen-rich layer with just one mass zone overlying a core of a fixed size. As in most cases of interest the hydrogen zone is geometrically thin and contains little mass, it is sufficient to consider a plane-parallel layer with a fixed gravitational acceleration g. The stellar structure equations may be written as

$$\frac{\partial P}{\partial \Sigma} = -g\,; \quad \frac{\partial P_r}{\partial \Sigma} = -\frac{\kappa F}{c}\,; \quad \frac{\partial F}{\partial \Sigma} = \epsilon - T\frac{DS}{Dt}\,; \qquad \frac{\partial z}{\partial \Sigma} = \frac{1}{\rho}\,; \quad \frac{\partial X}{\partial t} = -\frac{\epsilon}{E^*}\,, \tag{1}$$

where P is total pressure, P_r is radiation pressure, ρ is density, T is temperature, S is entropy, Σ is column mass density, t is time, F is radiative heat flux, ϵ is the nuclear energy generation rate, κ is opacity, c is the speed of light, and E^* is the energy released by burning 1 g of hydrogen. The boundary conditions at the top of our zone, i.e., at the stellar surface, are

$$\Sigma = \Sigma_s(t)\,, \quad P \approx 0\,, \quad P_r \approx 0\,, \quad X = X_s\,; \tag{2}$$

and the boundary conditions at the bottom of the shell are

$$\Sigma = \Sigma_b(t)\,, \quad F = F_b\,, \quad X = 0\,, \tag{3}$$

where F_b is the heat flux from the hydrogen-depleted core. The accretion rate $\dot{\Sigma}_a$ is related to Σ_s by

$$\frac{d\Sigma_s}{dt} = \dot{\Sigma}_a\,, \tag{4}$$

and the surface mass density of the whole zone is given as

$$\Delta\Sigma = \Sigma_s - \Sigma_b\,. \tag{5}$$

Equations (1) may be integrated over the whole hydrogen-rich zone to obtain

$$P = -g\int d\Sigma\,; \quad P_r = -\frac{1}{c}\int \kappa F d\Sigma\,; \quad F = \int\left(\epsilon - T\frac{DS}{Dt}\right)d\Sigma\,; \quad z = \int\frac{d\Sigma}{\rho}\,; \qquad \int\frac{DX}{Dt}\,d\Sigma = -\frac{1}{E^*}\int\epsilon d\Sigma\,. \tag{6}$$

So far our equations were pretty accurate, with only a few simplifications. Radiative equilibrium was assumed, and only the dominant terms were retained in the heat balance equation. Now we are going to make the most drastic simplification. We shall replace the functions under all integrals in equations (6) with their values at the bottom or top of the shell. In the last equation we shall effectively adopt a step-like profile of hydrogen distribution. Now, these equations may be written as

$$P = g\Delta\Sigma\,; \quad P_r = \frac{\kappa}{c}F\Delta\Sigma\,; \quad F = F_b + \left(\epsilon - T\frac{dS}{dt}\right)\Delta\Sigma\,; \quad \Delta z = \frac{\Delta\Sigma}{\rho}\,; \qquad X\frac{d(\Delta\Sigma)}{dt} - X\dot{\Sigma}_a = -\frac{\epsilon}{E^*}\Delta\Sigma\,, \tag{7}$$

where P, P_r, T, ρ, S, κ, ϵ refer to the values of corresponding physical quantities at the bottom of the shell, and X, F refer to the values at the surface. One may try to improve the accuracy of equations (7) by introducing some dimensionless factors, but this is not essential for this project. However, there is another simplification in the heat balance equation, where the derivative DS/Dt has been replaced with dS/dt. Fortunately, in most cases this does not introduce a very large error.

Equations (7) describe the conditions of hydrostatic equilibrium, radiative equilibrium, heat balance, a relation between the zone thickness its density and its surface mass density, and finally the mass balance. We effectively assume that matter falls onto the surface of our zone by accretion, and flows through the bottom of the one zone by nuclear burning. The one zone is neither Lagrangian nor Eulerian; it is confined to that layer that is rich in nuclear fuel, hydrogen in our case. The improper modification of the DS/Dt term results in a neglect of heat carried with matter flowing through the bottom of the one zone.

The set of equations (7) includes two ordinary differential equations which may be written as

$$T\frac{dS}{dt} = \epsilon - (F - F_b)\frac{g}{P}\,, \qquad \frac{dP}{dt} = g\dot{\Sigma}_a - \frac{\epsilon P}{XE^*}\,. \tag{8}$$

This set of equations may be integrated numerically provided that gravitational acceleration g, accretion rate $\dot{\Sigma}_a$, chemical composition of accreted matter X and Z, and the heat flux at the bottom of the shell F_b are all specified. I shall confine myself to the case when all these parameters are kept constant in any given model. Of course, it is necessary to know the equation of state, the opacity, and the nuclear burning rate as a function of density, temperature, and chemical composition.

We shall look first for steady-state solutions of equations (8), i.e., we shall keep $dS/dt = 0$, and

$dP/dt = 0$. We are left with algebraic equations which may be written as

$$F - F_b = \frac{\epsilon P}{g} = \epsilon \Delta\Sigma ,$$

$$\dot{\Sigma}_a = \frac{\epsilon P}{XE^* g} = \frac{\epsilon \Delta\Sigma}{XE^*} , \tag{9}$$

which may be combined to obtain

$$F - F_b = \dot{\Sigma}_a X E^* ; \tag{10}$$

i.e., the heat flux from the surface is equal to the heat flux from the core plus the heat released in a steady state nuclear burning.

Let us define a critical (i.e., Eddington) flux from the surface as

$$F_c \equiv cg/\kappa_e , \tag{11}$$

where κ_e is the electron scattering opacity. Let us define $1 - \beta$ as the ratio of radiation pressure to the total pressure. Combining equations (7), (10), and (11), we obtain

$$F = F_c \frac{\kappa_e}{\kappa} (1 - \beta) . \tag{12}$$

It is well known that while the luminosity of any stellar model increases the radiative pressure and electron scattering become dominant, i.e., $\beta \to 0$ and $\kappa \to \kappa_e$. The critical value may be approached but not exceeded by the luminosity as long as the condition of hydrostatic equilibrium is satisfied. In our plane-parallel model the radiation flux may approach but may not exceed F_c.

It is convenient to define a critical and a dimensionless accretion rate as

$$\dot{\Sigma}_c \equiv \frac{cg}{\kappa_e E^* X} , \quad \dot{a} \equiv \frac{\dot{\Sigma}_a}{\dot{\Sigma}_c} , \tag{13}$$

and a dimensionless heat flux from the core

$$f_b = F_b/F_c . \tag{14}$$

Now we may write the equations (8) as

$$T \frac{dS}{dt} = \epsilon + \frac{cg^2}{\kappa_e P} \left[f_b - \frac{\kappa_e}{\kappa} (1 - \beta) \right] ,$$

$$E^* X \frac{d \ln P}{dt} = -\epsilon + \frac{cg^2}{\kappa_e P} \dot{a} . \tag{15}$$

These differential equations must be supplemented with the following algebraic equations:

$$\kappa_e = 0.2(1 + X) , \quad 1 - \beta = \frac{P_r}{P} = \frac{aT^4}{3P} ,$$

$$P = P(\rho, T, X, Z) , \quad P_T = \frac{\partial \ln P}{\partial \ln T} , \quad P_\rho = \frac{\partial \ln P}{\partial \ln \rho} ,$$

$$\kappa = \kappa(\rho, T, X, Z) , \quad \kappa_T = \frac{\partial \ln \kappa}{\partial \ln T} , \quad \kappa_\rho = \frac{\partial \ln \kappa}{\partial \ln \rho} ,$$

$$\epsilon = \epsilon(\rho, T, X, Z) , \quad \epsilon_T = \frac{\partial \ln \epsilon}{\partial \ln T} , \quad \epsilon_\rho = \frac{\partial \ln \epsilon}{\partial \ln \rho} ,$$

$$dS = \frac{P}{\rho T} ds , \quad s_T = \frac{\partial s}{\partial \ln T} , \quad s_\rho = \frac{\partial s}{\partial \ln \rho} . \tag{16}$$

We shall study the properties of solutions of these equations for many models. First, we consider steady state nuclear burning. In that case the time derivatives in the equations (15) vanish, and we have two nonlinear algebraic equations instead:

$$\dot{a} + f_b = \frac{\kappa_e}{\kappa} (1 - \beta) ,$$

$$\epsilon P = \frac{cg^2}{\kappa_e} \dot{a} . \tag{17}$$

These may be solved when combined with equations (16). In general there is a discrete set of solutions for a given set of model parameters: $g, \dot{a}, f_b, X, Z$. The details of all the calculations will be given in the subsequent sections. Here I would like to present some examples of the results.

We shall consider various models with a logarithm of gravitational acceleration equal to 8.5. This corresponds to the surface conditions on a degenerate dwarf of 0.929 solar masses. The accreted matter will have a normal Population I composition: $X = 0.7$, $Z = 0.03$. Under these conditions the critical surface radiation flux is 2.8×10^{19} ergs cm^{-2} s^{-1}, the critical luminosity is 1.37×10^{38} ergs s^{-1}, and the critical accretion rate onto the whole surface is 3.3×10^{19} g s^{-1}. Most models will have a dimensionless heat flux from the core of 0.001, and a large range of dimensionless accretion rates. Notice, that the dimensionless radiative heat flux from the surface is given as $\dot{a} + f_b$. On all the figures the column density of hydrogen-rich zone is indicated as Σ rather than $\Delta\Sigma$.

The variation of column density with accretion rate is shown in Figure 1 for a number of values of heat flux from the core. Each line may be considered to display a linear series of stellar models (Gabriel and Ledoux 1967; Gabriel and Noels-Grotsch 1968; Paczyński 1972, 1980). Notice that a line with $F_b/F_c = 0.3$ varies monotonically. Other lines have several branches separated by turning points at which column mass density reaches a local maximum or minimum. According to general properties of linear series we may expect some branches to be thermally unstable.

Once we have models with steady-state nuclear burning, we may test them for stability with respect to small perturbations with exponential time dependence:

$$\delta \ln T = x \exp(\sigma t) ,$$

$$\delta \ln \rho = y \exp(\sigma t) \qquad |x| \ll 1 , \quad |y| \ll 1 . \tag{18}$$

All other perturbations may be expressed in terms of $\delta \ln T$ and $\delta \ln \rho$. A standard analysis applied to equations

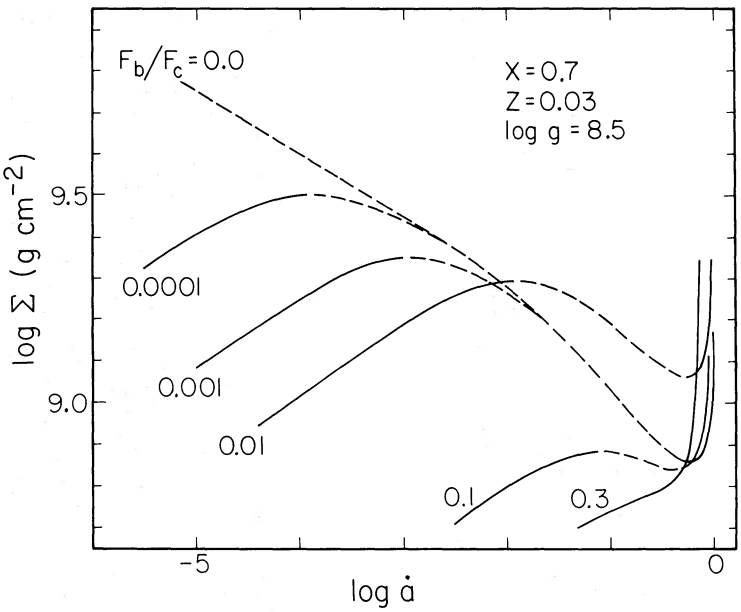

FIG. 1.—The variation of column density Σ of hydrogen-rich shell with dimensionless accretion rate is shown for degenerate dwarfs with a logarithm of surface gravity of 8.5 accreting matter with a composition: $X = 0.7$, $Z = 0.03$. Various lines are labeled with the values of dimensionless heat flux from hydrogen-depleted cores. Broken lines correspond to branches with unstable models. Notice that for $F_b/F_c > 0.17$ all models are stable.

(15) and (16) gives a quadratic equation for the eigenvalues

$$C_1\tau_n\tau_{\rm th}\sigma^2 + \{(C_1 + C_2)\tau_{\rm th} + [C_4(1+\alpha) - C_3]\tau_n\}\sigma + (C_3 + C_4 + C_5)(1+\alpha) = 0\,, \quad (19)$$

where

$$C_1 = s_T P_\rho - s_\rho P_T\,, \quad C_2 = s_T \epsilon_\rho - s_\rho \epsilon_T\,,$$
$$C_3 = \epsilon_T P_\rho - \epsilon_\rho P_T\,, \quad C_4 = P_T \kappa_\rho - P_\rho(\kappa_T - 4)\,,$$
$$C_5 = \epsilon_T \kappa_\rho - \epsilon_\rho(\kappa_T - 4)\,,$$
$$\alpha = \frac{f_b}{\dot a}\,, \quad \tau_n = \frac{E^* X}{\epsilon} = \frac{\Delta\Sigma}{\dot\Sigma_a}\,, \quad \tau_{\rm th} = \frac{P}{\rho\epsilon}\,. \quad (20)$$

Equation (19) provides us with two eigenvalues, σ_1 and σ_2. Their physical meaning becomes apparent when the two characteristic time scales, nuclear and thermal, are very different from each other. In that case equation (19) is equivalent to the two linear equations:

$$\sigma_{\rm th} = \tau_{\rm th}^{-1}[C_3 - C_4(1+\alpha)]/C_1\,,$$
$$\sigma_n = \tau_n^{-1}(C_3 + C_4 + C_5)(1+\alpha)/[C_3 - C_4(1+\alpha)]\,, \quad (21)$$

for $\tau_n/\tau_{\rm th} \gg 1$ and $|\sigma_n/\sigma_{\rm th}| \ll 1$.

Expressions (21) may also be obtained differently. If the first of equations (15) is perturbed in such a way that the column density of the hydrogen zone remains constant then the expression for $\sigma_{\rm th}$ is obtained. This is equivalent to a standard thermal stability analysis, with the distribution of chemical composition unperturbed. It is reasonable while the thermal time scale, and presumably the time scale of the perturbation, is much shorter than nuclear time scale. Notice that in our model constant column density implies constant pressure, and the perturbation is isobaric. If the second of equations (15) is perturbed adiabatically, then the expression for σ_n is obtained.

Let us consider now a linear series of steady-state models with accretion rate changing along the series. The two equations (17) must be satisfied, and we obtain the relation

$$d\ln(\Delta\Sigma) = d\ln P = \frac{C_3 - C_4(1+\alpha)}{(C_3 + C_4 + C_5)(1+\alpha)}\, d\ln \dot a\,, \quad (22)$$

which holds along the series. Comparison of equations (21) and (22) demonstrates that a local maximum or minimum of column density, i.e., a turning point of a linear series, coincides with a point at which the thermal eigenvalue $\sigma_{\rm th}$ passes through zero. The corresponding model is marginally stable. This is a usual relationship between the turning points of linear series and the onset of thermal stability or instability (Paczyński 1980 and references therein). However, it is clear that this relation may only be approximate, as it is a consequence of a simplification which led to equations (21).

At a turning point of a linear series the nuclear eigenvalue diverges (cf. eq. [21]) while the thermal eigenvalue passes through zero. Therefore, within some region close to a turning point the two eigenvalues must be of the same order of magnitude, and the conditions required for equations (21) are not satisfied. In that region the coupling between the two equations (15)

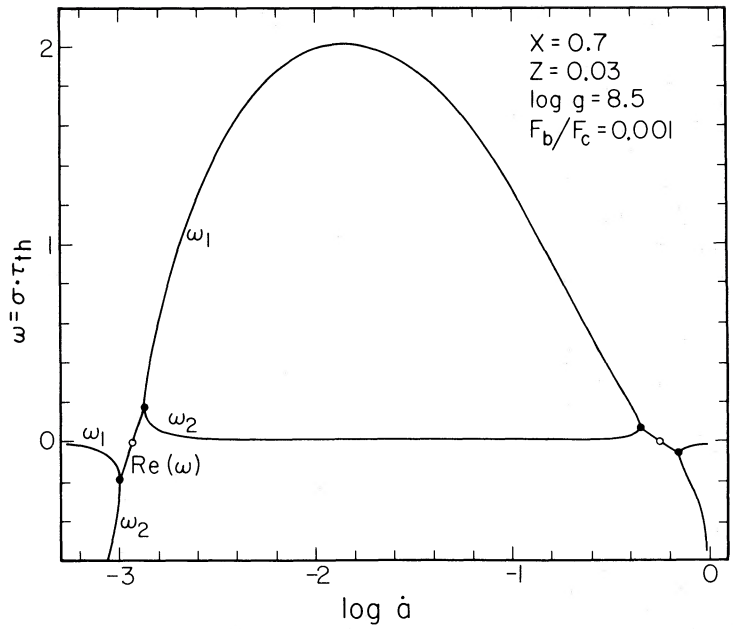

FIG. 2.—The variation of real eigenvalues (or a real part of complex eigenvalues) with dimensionless accretion rate is shown for a degenerate dwarf with a logarithm of surface gravity equal 8.5, and dimensionless heat flux from the hydrogen-depleted core of 0.001, accreting matter with a composition: $X = 0.7$, $Z = 0.03$. The region between the two open circles has positive eigenvalues, and the models are unstable there. The corresponding branch of the linear series of models is shown with a broken line in Fig. 1.

becomes strong and it is necessary to calculate the two eigenvalues with the quadratic equation (19). It may be shown that the two eigenvalues become complex in that region.

The variation of the two eigenvalues along a series of models is shown in Figures 2 and 3. The variation of column density along this sequence was shown in Figure 1. The dimensionless eigenvalues are defined as

$$\omega_{1,2,\mathrm{th},n} = \tau_{\mathrm{th}}^{-1}\sigma_{1,2,\mathrm{th},n} \,. \tag{23}$$

Transition from thermal stability to instability is indicated by the real part of the eigenvalues calculated with equation (19) passing through zero. This is close to the place where the thermal eigenvalue goes through zero (cf. Fig. 3). Therefore, marginal thermal stability nearly coincides with a turning point of a linear series.

Given an unstable steady-state model, we would like to ascertain the development of instability in the nonlinear regime. This may be found by numerical integrations of the two differential equations (15). An example of that is shown in Figure 4 for a model with a dimensionless accretion rate of 0.01, located on the unstable branch of a linear series shown in Figure 1 and labeled $F_b/F_c = 0.001$. According to Figure 2 this model is unstable. Numerical integrations of equations (15) demonstrated a rapid development of large-amplitude relaxation oscillations, with a period of 790 years. The variation of density and pressure throughout the flash cycle of this model is shown in Figure 5, together with density and pressure variations along a linear series of steady-state stellar models with $F_b/F_c = 0.001$. Notice that in a "high" state of the flash cycle, when

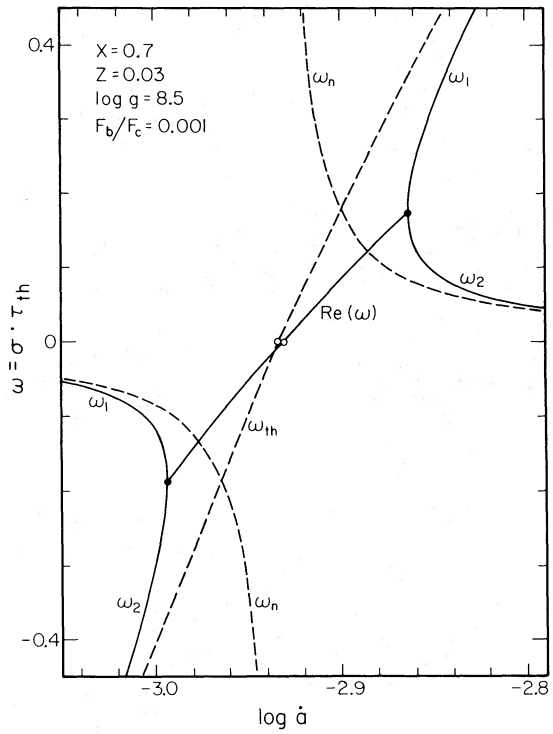

FIG. 3.—A blow-up of a part of Fig. 2. The dashed lines indicate the thermal and nuclear eigenvalues calculated with eqs. (21). The solid lines indicate the eigenvalues (or a real part of complex eigenvalues) calculated with equation (19). Notice that the transition from stability to instability ($\omega = 0$) is almost at the same place for the dashed and solid lines, and that the two types of lines are very close to each other far from the point of marginal stability.

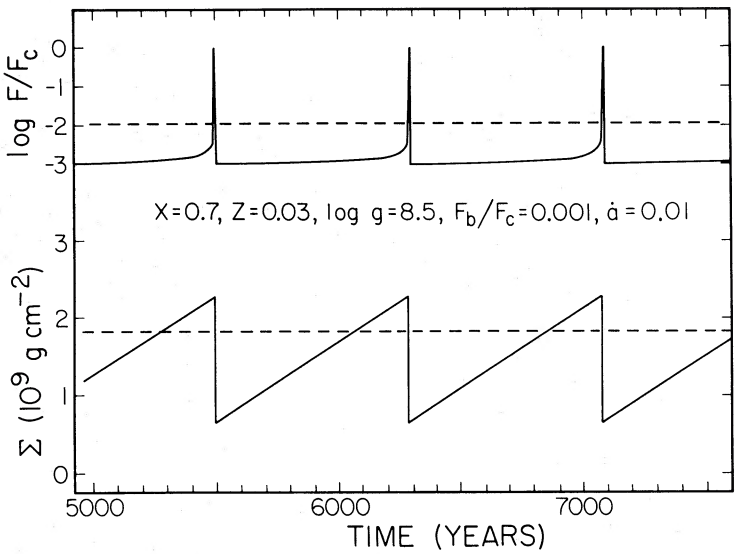

FIG. 4.—The variation with time of the dimensionless surface radiation flux F/F_c, and column density of hydrogen-rich zone Σ, for a degenerate dwarf with a logarithm of surface gravity equal 8.5 (corresponding to 0.929 $M_\odot$), accreting matter with a composition: $X = 0.7$, $Z = 0.03$. The critical radiation flux for this model is 2.8×10^{19} ergs cm^{-2} s^{-1}, the corresponding critical luminosity is 1.37×10^{38} ergs s^{-1}, and the critical accretion rate onto a whole star is 3.3×10^{19} g s^{-1}. The dimensionless heat flux from the hydrogen-depleted core is 0.001, and the dimensionless accretion rate is 0.01, which corresponds to $\dot{M} = 3.3 \times 10^{17}$ g s^{-1}. The surface flux and surface mass density corresponding to the equilibrium model with a steady-state nuclear burning are shown with horizontal dashed lines. The flash cycle period is 790 years.

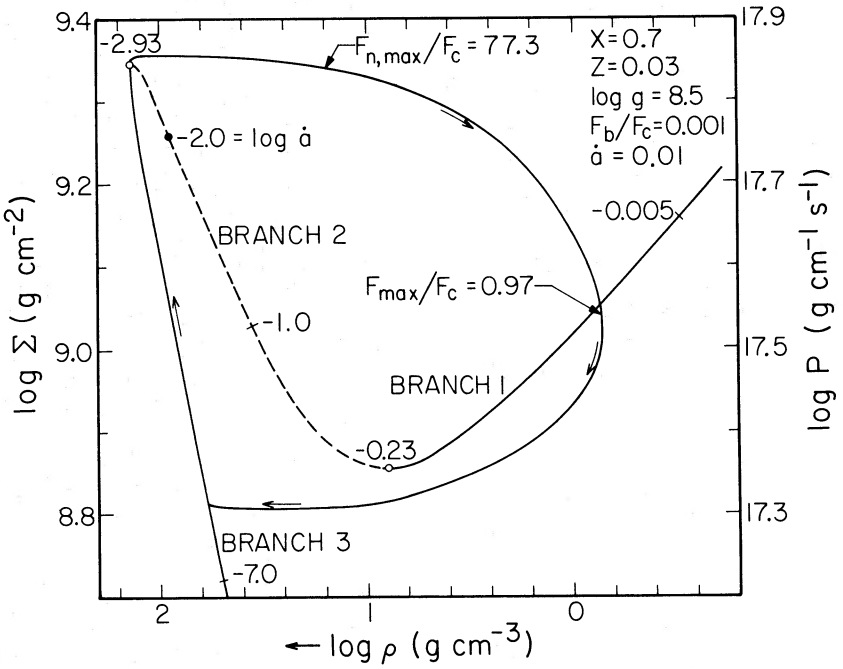

FIG. 5.—The variation of surface mass density Σ and density ρ in the hydrogen burning zone throughout a flash cycle is shown with a closed loop with arrows for the model shown in Fig. 4. The position of the equilibrium model with a steady-state nuclear burning is shown with a large dot. Also shown are three branches of the equilibrium models with dimensionless accretion rate ranging from $10^{-0.005}$ to $10^{-0.23}$ on branch 1, from $10^{-0.23}$ to $10^{-2.93}$ on branch 2, and from $10^{-2.93}$ to $10^{-7.0}$ on branch 3. Models on branches 1 and 3 are stable, while those on branch 2 are unstable. Notice that pressure at the bottom of hydrogen zone is given as $P = g\Sigma$.

hydrogen is burning, the model evolves close to the first branch of the linear series. In a "low" state, when hydrogen burning is switched off, the model evolves along the third branch. This is very similar to the finding of Barranco, Buchler, and Livio (1980, Fig. 1).

III. HYDROGEN ACCRETION ONTO DEGENERATE DWARFS

I used simple approximate formulae to describe the properties of hydrogen rich matter, i.e., pressure P, internal energy U, opacity κ, and nuclear energy generation rate ϵ:

$$P_r = \frac{a}{3} T^4 , \quad P = P_r + \frac{k}{\mu H} \rho T + K\rho^{5/3} ,$$

$$\frac{1}{\mu} = 2X + 0.75Y + 0.5Z = 0.75 + 1.25X - 0.25Z ,$$

$$K = 3.12 \times 10^{12}(1 + X)^{5/3} ,$$

$$U = \frac{aT^4}{\rho} + \frac{3}{2}\frac{k}{\mu H} T + \tfrac{3}{2} K\rho^{2/3} ,$$

$$\kappa = 0.2(1 + X)\left[1 + 2 \times 10^{26}(0.001 + Z)\frac{\rho}{T^{3.5}}\right] ,$$

$$\epsilon = \epsilon_{CN} = 8 \times 10^{27} X X_{CN} \rho T_6^{-2/3} \times \exp\left(-152.313 T_6^{-1/3}\right) ,$$

$$T_6 = T/10^6 , \quad X_{CN} = Z/3 , \quad E^* = 6 \times 10^{18} \text{ ergs g}^{-1} ,$$

$$\dot{\Sigma}_c \equiv \frac{cg}{\kappa_e E^* X} = \frac{2.5 \times 10^{-8}}{X(1 + X)} g \text{ g cm}^{-2} \text{ s}^{-1} ,$$

$$F_c = \frac{1.50 \times 10^{11}}{(1 + X)} g \text{ ergs cm}^{-2} \text{ s}^{-1} . \qquad (24)$$

These determine uniquely all the quantities in equations (16), and make the analysis of equations (17), (20), and the numerical integrations of equations (15) possible. Some results were already presented in the preceding chapter. Those were the examples of linear series of steady state models (Fig. 1), the variation of eigenvalues along one such series (Figs. 2 and 4), and an example of full-amplitude shell flashes for one model on that series (Figs. 4 and 5). All those computations were done for a logarithm of gravitational acceleration equal to 8.5, which corresponds to a degenerate dwarf of 0.929 $M_\odot$.

In this section I shall present the results of one zone model computations for a large range of parameters. Surface gravity will be varied from $10^{7.5}$ to $10^{9.5}$ cm s^{-2}, which corresponds to degenerate dwarfs ranging from 0.336 to 1.373 $M_\odot$. The line separating stable and unstable models in the (f_b, $\dot{a}$)-plane [i.e., in the heat flux from the (core, accretion rate)-plane] is shown in Figures 6 and 7 for models with various chemical compositions and gravitational accelerations. All the curves of marginal stability are similar. In all cases the unstable models are to the left of the lines. Notice that if the heat flux from the core is above some critical value, then models are stable for any value of the accretion rate. If the heat flux from the core is below the critical value, then models are stable for very high and for very low accretion rates, and they are unstable for the intermediate rates. The transition from stability to instability is little affected when the opacity is assumed to be due to electron scattering only and the effect of electron degeneracy is neglected, as seen in Figure 6.

The influence of metal content on the stability is systematic but small (cf. Fig. 6). However, when the metal content was taken as zero and the proton-proton cycle was the only source of nuclear energy, then all models were found to be stable. The stability lines as presented in Figure 6 are most likely incorrect for models with a very low metal content, as the energy generation rate due to the CNO cycle may be limited with beta decays. The stability was little affected by variation of hydrogen content, unless the variation was very large (cf. Fig. 7). The effect of gravity was small but systematic. In general, the range of unstable models increased when the metal and hydrogen contents were increased and when the gravitational acceleration was decreased.

The one-zone model offers a possibility to calculate a period of shell flash cycles, like those shown in Figure 4. The variation of that period with the accretion rate is shown in Figure 8 for models with a Population I composition, a logarithm of gravitational acceleration equal to 8.5, and for various values of heat flux from the core. Notice that the period is roughly inversely proportional to the accretion rate, and it decreases with increasing heat flux from the core. The variation of flash cycle period with gravity is shown in Figure 9 for many values of accretion rate and heat flux from the core. The $\dot{a}_{max}$ corresponds to the largest accretion rate at which the models were still unstable. That was about 0.5 for $F_b = 0$, and about 0.4 for $F_b/F_c = 0.1$. Notice that the shortest flash cycle was only 1 month long, for log $g = 9.5$, $F_b/F_c = 0.1$, $\dot{a} = \dot{a}_{max} \approx 0.35$. This corresponds to a white dwarf of 1.373 $M_\odot$ accreting at a rate of 2.7×10^{-7} $M_\odot$ per year. On average it would radiate about 1.8×10^4 $L_\odot$, i.e., about 40% of the output from a red giant of the same core mass.

It is interesting to look for a relationship between the period of nuclear shell flashes and some other time scales which may be calculated with less effort. One such characteristic time scale may be nuclear, i.e., τ_n as defined by the last of equations (20). Another may be a period of small-amplitude oscillations which may be readily calculated for marginally stable models as $2\pi/\text{Im}(\sigma)$. The three time scales are shown in Figure 10 for marginally unstable models with a logarithm of gravitational acceleration equal to 8.5 and with Population I composition. These models correspond to the lines of marginal stability shown in Figures 6 and 7. The three nearly horizontal lines at the bottom of Figure 10 correspond to high accretion rates, and therefore they correspond to the nearly horizontal marginal stability lines at the top of Figures 6 and 7. The three inclined lines in Figure 10 correspond to low accretion rates and to the inclined marginal stability lines in Figure 6 and 7.

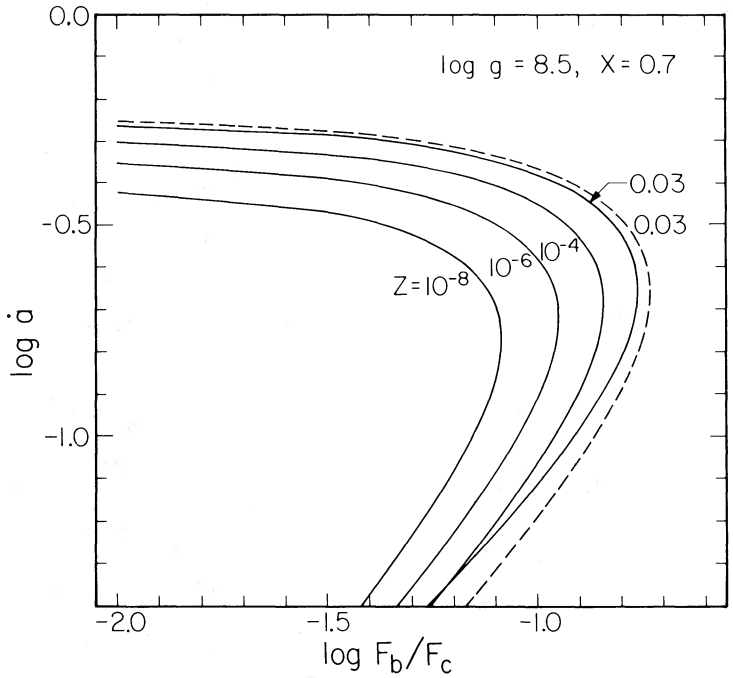

FIG. 6.—The variation of dimensionless accretion rate with dimensionless heat flux from hydrogen-depleted cores is shown for marginally stable models of accreting and hydrogen-burning degenerate dwarfs with a logarithm of surface gravity equal to 8.5. Hydrogen content of accreted matter is $X = 0.7$, and metal content Z is shown for each line separately. The dashed line corresponds to a model with opacity due to Thomson electron scattering only, and with the pressure of degenerate electrons neglected. The unstable models are to the left of each line.

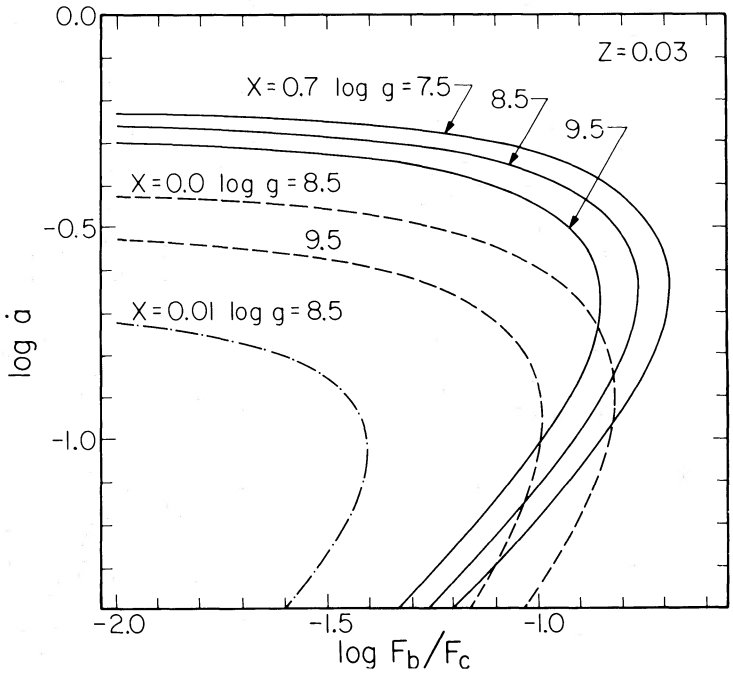

FIG. 7.—The same as Fig. 6, but for different chemical compositions of accreting matter, and different surface gravities

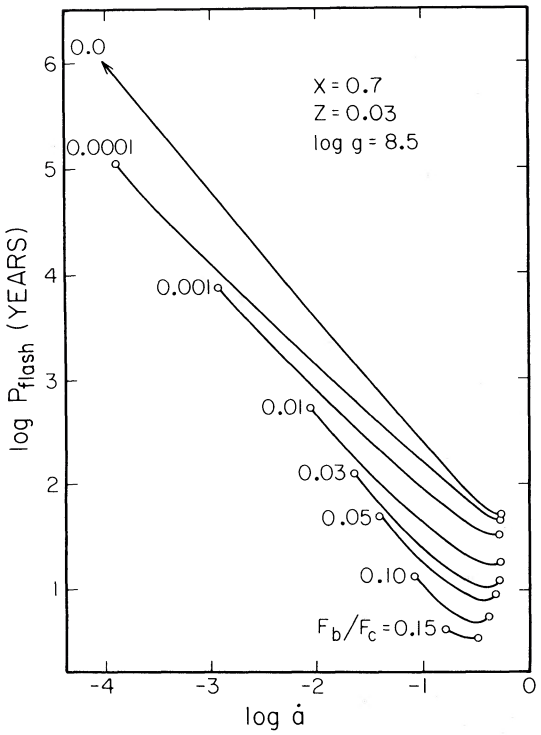

FIG. 8.—The variation of a shell flash period with dimensionless accretion rate for degenerate dwarfs with a logarithm of surface gravity equal to 8.5, accreting matter with a composition $X = 0.7$, $Z = 0.03$. The curves are labeled with the values of dimensionless heat flux from hydrogen-depleted cores. Marginally unstable models are indicated with open circles at the ends of the curves.

Notice that the flash period is usually more than an order of magnitude longer than the corresponding period of small-amplitude oscillations. At small accretion rates (and therefore small F_b) the duration of flash cycles is rather similar to the corresponding nuclear time scales. However, this is not the case at the highest accretion rates, for which the flash cycles are almost an order of magnitude longer than the corresponding nuclear time scales, as indicated by the nearly horizontal lines at the bottom of Figure 10. Therefore, one should be careful with estimates of the duration of flash cycles which are not based on nonlinear development of shell instability.

IV. HELIUM ACCRETION ONTO DEGENERATE DWARFS

Models accreting helium differed from those accreting hydrogen, as the carbon-nitrogen cycle was replaced with the triple-alpha reaction,

$$\epsilon = \epsilon_{3\alpha} = 3.5 \times 10^{11} Y^3 \rho^2 T_8^{-3} \exp(-43.2/T_8),$$
$$T_8 = T/10^8, \quad Y = 1 - X - Z,$$
$$E^* = 5.8 \times 10^{17} \text{ ergs g}^{-1},$$
$$\dot{\Sigma}_c \equiv \frac{cg}{\kappa_e E^* Y} = 2.7 \times 10^{-7} g \text{ g cm}^{-2} \text{ s}^{-1},$$
$$F_c = 1.50 \times 10^{11} g \text{ ergs cm}^{-2} \text{ s}^{-1}. \quad (25)$$

All the formulae for equation of state and opacity remained the same as those given with equations (24).

All the models had zero hydrogen content and $Z = 0.03$, and therefore $Y = 0.97$. The lines of marginal stability are shown in Figure 7 in the $(\dot{a}, f_b)$-plane. They are very similar to the corresponding lines for hydrogen-rich models. The helium shell flashes were computed for many models with a gravitational acceleration ranging from 10^8 to $10^{9.5}$ cm s^{-2}, which corresponds to degenerate dwarfs ranging from 0.595 to 1.373 $M_\odot$. Models with smaller masses (and gravities) would not justify the assumption that the helium-rich zone had a thickness much smaller than the stellar radius. All qualitative properties of helium shell flashes are similar to those of hydrogen shell flashes, but the flash cycle periods are much longer, approximately a factor of 10. The variation of the flash period with gravity is shown in Figure 11 for helium models. This may be compared with Figure 9 showing the same relations for hydrogen-rich models.

V. HELIUM ACCRETION ONTO NEUTRON STARS

These models had identical nuclear burning rate, equation of state, and opacity as the models presented in the previous chapter, but gravitational acceleration

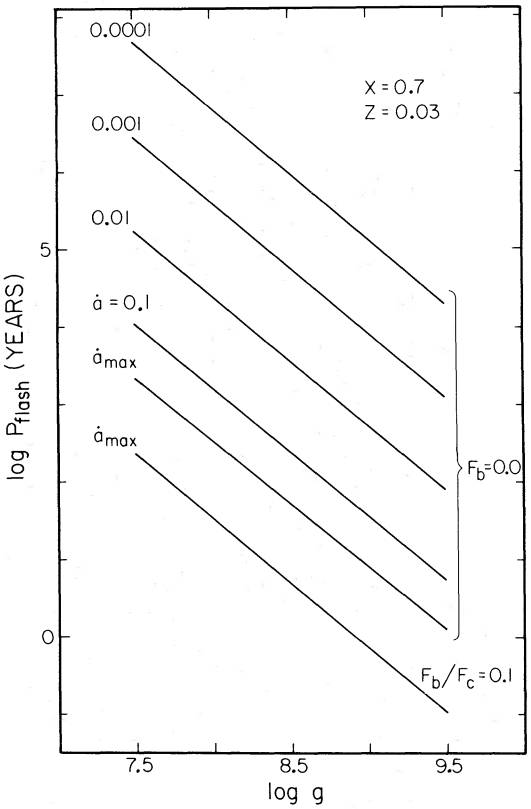

FIG. 9.—The variation of a shell flash period with a logarithm of surface gravity for degenerate dwarfs accreting matter with a composition: $X = 0.7$, $Z = 0.03$. The lines are labeled with values of dimensionless accretion rate and heat flux from hydrogen-depleted cores.

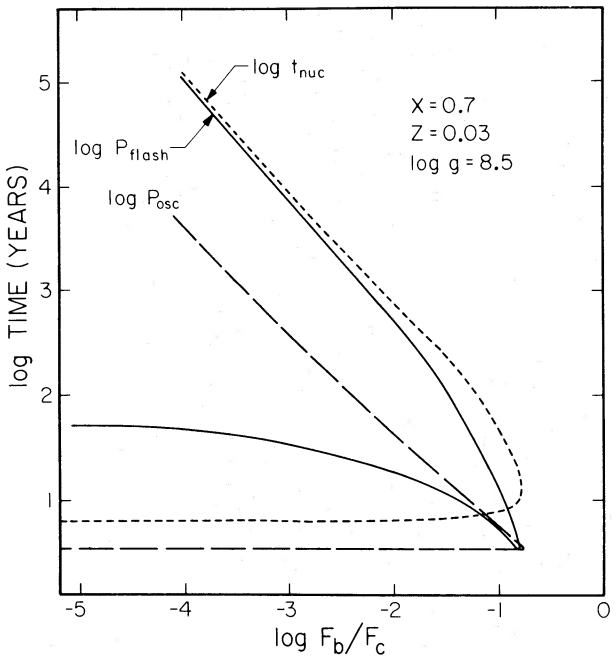

FIG. 10.—The variation of a period of small-amplitude oscillations P_{osc}, a period of a full-amplitude flash cycle P_{flash}, and a nuclear time scale $t_{nuc} = E^*X/\epsilon$ (cf. eqs. [20]), with dimensionless heat flux from hydrogen-depleted cores is shown for marginally unstable models. The logarithm of surface gravity is 8.5, and the accreted matter has a composition: $X = 0.7$, $Z = 0.03$. The accretion rate corresponding to various values of heat flux from the core, F_b/F_c, may be found from Fig. 6 or 7.

was much larger. It ranged from 10^{14} to 10^{15} cm s^{-2}, which was appropriate for a neutron star surface. The lines of marginal stability in the $(\dot{a}, f_b)$-plane are shown in Figure 12. They are similar to those shown in Figures 6 and 7, but they are strongly displaced down and to the left. Again, qualitative properties of shell flashes are very much like those in the two previous sections, but all the characteristic time scales are much shorter now. The periods of small-amplitude oscillations are shown for marginally unstable models in Figure 12. Notice that these periods are now measured in seconds, not in years as in the previous sections. Of course, the periods of nonlinear flash cycles are somewhat longer.

It should be pointed out that our definition of a critical accretion rate (cf. eq. [13]) is not very relevant for neutron stars. It was reasonable for degenerate dwarfs, because in that case most of energy released in accretion was nuclear, not gravitational. The opposite is true for neutron stars, for which the gravitational energy of accreted matter is about two orders of magnitude larger than that due to helium burning. Therefore, $\log \dot{a} \approx -2$ in Figure 12 corresponds to a critical (Eddington) luminosity due to release of gravitational energy, presumably in a shock above the stellar surface, beyond our one-zone model. It follows that our dimensionless accretion rate $\dot{a} \approx 0.01$ roughly corresponds to the critical rate for neutron stars. When this is taken into account, we find that the difference between Figure 12 and Figures 6 and 7 is reduced substantially.

Unfortunately, the range of applicability of the one-zone model to the accreting neutron stars is rather limited. The results presented in Figure 12 are based on computations which ignored electron thermal conductivity. This becomes important when electron degeneracy becomes appreciable, and this corresponds to an accretion rate below 10^{-4} of the critical rate. In this regime the results change dramatically as soon as electron conductivity is taken into account. There are large areas in the $(\dot{a}, f_b)$-plane in which no steady-state models can be found, while in other areas multiple solutions exist. The main problem is due to the decrease of effective opacity (or increase of effective conductivity) at the bottom of the accreted zone. In fact, the opacity may change non-monotonically with depth, making our one-zone approximation improper. I shall not discuss these complications in more detail, as it would be beyond the scope of this simple presentation. Fortunately, electron conductivity was not important for one-zone models of accreting white dwarfs within the range of parameters presented in this paper.

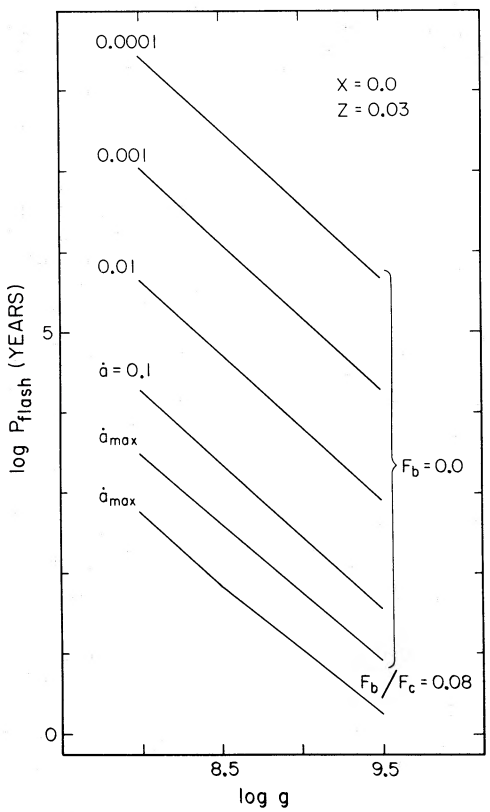

FIG. 11.—The variation of a shell flash period with a logarithm of surface gravity for degenerate dwarfs accreting helium-rich matter with a composition: $X = 0.0$, $Z = 0.03$. The lines are labeled with values of dimensionless accretion rate and heat flux from helium-depleted cores.

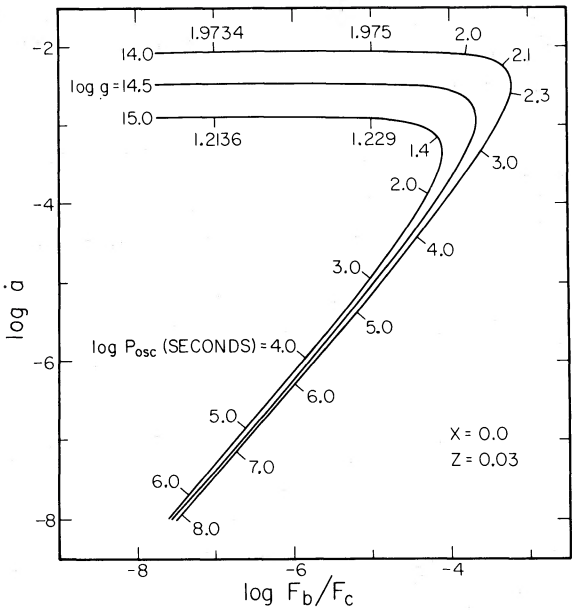

FIG. 12.—The variation of dimensionless accretion rate with dimensionless heat flux from helium-depleted cores is shown for marginally unstable models of neutron stars accreting helium-rich matter with a composition: $X = 0.0$, $Z = 0.03$. The curves are labeled with values of a logarithm of surface gravity: 14.0, 14.5, and 15.0. A period of small-amplitude oscillations is shown along two curves. Full-scale flash cycles have longer periods. Electron conductivity was not taken into account, and this limits the validity of this diagram to dimensionless accretion rates exceeding 10^{-4}.

VI. DISCUSSION

The one-zone model presented in this paper allows a simple analysis of nuclear burning on accreting degenerate dwarfs and neutron stars. Some gross properties of such objects may be calculated with little effort and very small computer requirements. This makes it useful for pilot studies, for a qualitative analysis, and for teaching purposes. Because of its simplicity many details of real shell flashes cannot be obtained, and of course the accuracy of results is limited. However, many properties of shell flashes are reproduced surprisingly well.

We proceed by specifying the parameters needed for a model: gravitational acceleration at the stellar surface, accretion rate, composition of accreted matter, and the heat flux flowing from the stellar core into the accreted layer. Once these parameters are specified, a model with a steady-state nuclear burning may be calculated, provided the accretion rate and the heat flux from the core do not exceed some critical value, $\dot{a} + f_b < 1$ (cf. eq. [17]). The stability of a steady-state model against small amplitude perturbations may be analyzed. Finally, in the case of unstable models, numerical integration of the evolution into nonlinear regime can be easily done, as only two ordinary first order differential equations (15) are involved. I found that the general properties of the models were very similar for most chemical compositions of accreted matter, for degenerate dwarfs and for neutron stars alike. The only exception was accretion of hydrogen-rich matter with no metals onto white dwarfs. In that case the only nuclear reactions were those of the proton-proton cycle, and all models were found to be stable. I shall discuss now the common properties of all other models.

A linear series of stellar models with a steady-state nuclear burning may be calculated by varying the accretion rate and keeping all other model parameters constant (g, f_b, X, Z). For each value of accretion rate we may compute many characteristics of the one-zone model, in particular a column density. In general there are three branches of the linear series separated by two turning points at which the column density reaches a local minimum or maximum (cf. Fig. 1). The middle branch, located between the two turning points, is thermally unstable. Along this branch, column density decreases with increasing accretion rate. The other two branches are stable, with column density increasing with accretion rate. It follows that the models are stable when the accretion rate is high, close to the critical value (cf. eq. [13]), or very low, so that the rate at which heat is relased in nuclear reactions is lower than the heat flow from the core. This picture changes gradually while the heat flux from the core is increased. The unstable branch of the linear series becomes shorter and disappears completely when the heat flux from the core exceeds some critical value. In that case the models are stable for any value of accretion rate (cf. Figs. 6, 7, and 12). In their recent paper Papaloizou, Pringle, and MacDonald (1982) also point out that the increase of column density with increasing accretion rate is required for stability.

While we move along a linear series, the transition from stability to instability is always similar. Far from the marginal stability point the two eigenvalues are negative and differ considerably from each other. They are roughly equal to the inverse of the thermal and nuclear time scales, respectively. Any small perturbation decays exponentially. When we come closer to the point of marginal stability, the two eigenvalues first become equal to each other and later become complex, with the real part negative. A small perturbation oscillates with decreasing amplitude, and the models are still stable. Eventually the real part of the eigenvalues passes through zero and becomes positive. Small perturbations oscillate with increasing amplitude, and the models become unstable. Finally, the two eigenvalues become real and positive. Small perturbations grow exponentially. Far away from the point of marginal stability the two eigenvalues differ considerably from each other. They are roughly equal to the inverse of the thermal and nuclear time scales, respectively. This type of transition from stability to instability is similar to that found by Schwarzschild and Härm (1965) in their evolutionary computations leading to helium shell flashes on the red-giant asymptotic branch. In the case of one-zone model the point of marginal stability is close to the point where the "thermal eigenvalue" passes through zero (cf. Figs. 2

and 3), i.e., where the linear series has a turning point. Therefore, even a very simplified stability analysis based on the linear series approach (cf. Paczyński 1980 and references therein) is reasonably accurate, as the transition from stability to instability is very close to the turning point.

The two marginal stability lines shown in Figure 6 for $Z = 0.03$ make it clear that they are not significantly different in the cases when either more or less complicated formulae are used for the equation of state and opacity. Therefore, it is useful to present simplified formulae for the "thermal" and "nuclear" eigenvalues which may be obtained if pressure is just a sum of the pressures due to radiation and perfect, fully ionized gas, with no allowance made for electron degeneracy, while the opacity is due to Thomson electron scattering only. In this case equations (21) may be written as

$$\sigma_{\rm th} = \tau_{\rm th}^{-1} \frac{\beta(\nu - 1 - 4\alpha) - 4}{16 - 12\beta - 1.5\beta^2}, \qquad \sigma_n = \tau_n^{-1} \frac{\beta(\nu + 7)(1 + \alpha)}{\beta(\nu - 1 - 4\alpha) - 4}, \tag{26}$$

where

$$\nu = \partial \ln \epsilon / \partial \ln T, \quad \alpha = f_b/\dot{a}, \quad 1 - \beta = P_r/P = \dot{a} + f_b. \tag{27}$$

When the accretion rate is very high, $\dot{a} \approx 1$, then the temperature and luminosity are high, β and ν are small, and $\sigma_{\rm th}$ and σ_n are both negative. When the accretion rate is very low, $\dot{a} < f_b$, then α is large and again the two eigenvalues are negative, implying thermal stability of the one-zone model. However, if the heat flux from the core is small, $f_b \ll 1$, then there is a range of accretion rates for which the two eigenvalues are positive and the models are unstable. A similarly simplified analysis can be done for the eigenvalues following from the quadratic equation (19), and it can be shown that the transition from stability to instability proceeds through complex eigenvalues, just as it is seen in Figures 2 and 3 for the case of more complicated equation of state and opacity.

The nonlinear development of instability may be studied by means of numerical integrations of the two ordinary differential equations (15). The final behavior is the same for models which have oscillatory or exponential increase of small perturbations. The models evolve to large amplitude relaxation oscillations (cf. Fig. 4). Nuclear burning proceeds in short bursts separated by relatively long periods of no burning at all. During the flash the surface radiation flux is close to the critical (Eddington) value. When almost all nuclear fuel is used up, the burning is extinguished and the model cools off. The radiative heat flux from the surface drops to the minimum level equal to the heat flux from the core. Gradually, the surface mass density of our zone increases due to accretion, and so does the optical thickness of the accreted layer. As the radiative flux stays constant at its minimum level, the temperature at the base of accreted zone increases, and at some point the nuclear fuel is ignited. The instability develops very rapidly. Initially, the rate of heat release in nuclear burning increases so much that it exceeds the critical (Eddington) value by a large factor (cf. Fig. 5, the point with $F_{n,\max}/F_c = 77.3$). This energy is used mainly to heat up the accreted matter. The pressure remains constant as long as the amount of burned fuel is small ($P = g\Sigma$). The increase of temperature is accompanied by the decrease of density and the increase of geometrical thickness of the zone. The opacity declines and reaches the level of Thomson electron scattering. The radiation flux from the surface comes close to the Eddington limit (cf. Fig. 5, the point with $F_{\max}/F_c = 0.97$). A phase of stable nuclear burning follows. The mass of accreted zone gradually decreases, and the model evolves parallel to the first branch of a linear series (cf. Fig. 5). When column density is reduced below the value corresponding to the turning point of the linear series, then nuclear burning rapidly switches off. The unburned matter left in the accreted zone cools off and settles down close to the third branch of the linear series. We are at the beginning of the next cycle.

This picture changes somewhat when the heat flux from the core is very small or vanishes. In that case the matter in the accreted zone gradually heats up by compression while its mass increases, but the radiation leaking from the surface makes this process non-adiabatic. Therefore, in the case of negligible heat flux from the core as well as in the case when that heat flux is relatively large, the temperature at the base of accreted zone is higher if it is more difficult for radiation to diffuse out, i.e., if the opacity is large. Except for the details of heating between the flashes, there is not much difference between the two cases.

Throughout these computations a radiative heat diffusion was assumed. There is only one phase of every flash cycle during which almost entire accreted layer becomes convective. This is close to the peak of the flash, when the rate of heat release in nuclear burning exceeds the Eddington luminosity. However, almost all that heat is used to increase the entropy of accreted and burning matter, and only a very small fraction diffuses out and is radiated away from the surface. Therefore, the one-zone model describes reasonably the heating of matter, but provides somewhat incorrect account of the time variation of the surface luminosity during this very brief phase. As soon as the heat wave reaches the surface and the luminosity becomes close to the Eddington limit, the convection vanishes (cf. Paczyński and Żytkow 1978). Therefore, the one-zone model does not properly describe the rapid rise of surface luminosity, but provides a good description of a much longer phase of high luminosity and its gradual decline.

It should be pointed out that the one-zone model is plane-parallel, and because of this the maximum surface luminosity may become very close to the Eddington limit (i.e., critical luminosity). In case of a more proper spherically symmetric model the maximum surface luminosity would be that given by the core mass-

luminosity relation for red giants with degenerate cores (Paczyński and Żytkow 1978; Paczyński 1970). The two relations are gives as

$$L_{\rm Eddington} = \frac{4\pi cG}{\kappa_{el}} M = \frac{65{,}000}{1+X} L_\odot \frac{M}{M_\odot}, \quad (28a)$$

$$L_{\rm Red\ giant} = 59{,}250\, L_\odot (M/M_\odot - 0.522), \quad \text{for } X = 0.7, \quad Z = 0.03 . \quad (28b)$$

Our critical accretion rate (cf. eq. [13]) corresponds to the Eddington luminosity. In more realistic spherically symmetric models the maximum accretion rate for which the steady-state solutions exist would correspond to the red giant luminosity, and would be lower than that given with equation (13) by the ratio of equations (28a) and (28b).

The duration of a full-amplitude flash cycle may be readily obtained by integrating the equations (15). Usually, a full amplitude and a constant time interval between the flashes are reached within two or three flash cycles. These time intervals obtained with the one-zone model may be compared with those which followed from the full-scale evolutionary computations by Paczyński and Żytkow (1978). Those were done for a degenerate dwarf of 0.8 $M_\odot$ accreting matter with a composition $X = 0.7$, $Z = 0.03$. The minimum surface radius of those models was 0.0112 $R_\odot$ (i.e., 7.8×10^8 cm), somewhat larger than that of a zero-temperature degenerate dwarf of the same mass. A logarithm of gravitational acceleration at the surface was 8.24. The heat flux from the core was very small, 0.03 $L_\odot$. The calculated logarithms of interflash periods (in years) were 7.08, 5.09, 3.68, 2.90, and 2.14 for the accretion rates of 1.46×10^{-11}, 1.46×10^{-9}, 1.46×10^{-8}, 4.37×10^{-8}, and 1.067×10^{-7} $M_\odot$ yr^{-1}, respectively. One-zone models with $\log g = 8.24, f_b = 0.0, X = 0.7, Z = 0.03$, and all the physics described with equations (24) were calculated for comparison. The critical accretion rate for those models was $\dot{\Sigma}_c = 3.65$ g cm^{-2} s^{-1}; i.e., the rate for the whole star was $\dot{M}_c = 2.80 \times 10^{19}$ g s^{-1} = 4.44×10^{-7} $M_\odot$ yr^{-1}. The logarithms of dimensionless accretion rates corresponding to those used by Paczyński and Żytkow (1978) were -4.48, -2.48, -1.48, -1.01, and -0.62. The logarithms of interflash periods calculated with the one-zone models for these accretion rates were (in years): 7.03, 4.59, 3.40, 2.85, and 2.42, respectively. The agreement with the results of full-scale evolutionary computations is reasonably good, the differences never exceeding a factor of 3 for the periods, or 0.5 for the logarithms. There is a relatively large discrepancy for the highest accretion rate, 1.067×10^{-7} $M_\odot$ yr^{-1}, which corresponds to $\log \dot{a} = -0.62$. This highest rate corresponds to the marginally unstable model of Paczyński and Żytkow (1978). The marginally unstable one-zone model is found for $\log \dot{a} = -0.246$, with a logarithm of the corresponding flash period equal to 2.14 (in years). This is the shortest period for the models with the parameters specified above, and it is equal to the shortest period found with the full-scale evolutionary computations. It looks as if the periods of shell flashes calculated with the one-zone model are reasonable.

The shortest hydrogen shell flash cycle period possible for degenerate dwarfs accreting hydrogen rich matter is about 1 month (cf. Fig. 9). The shortest period for helium shell flashes on degenerate dwarfs is about 1 year (cf. Fig. 11). These results may be of interest for the studies of cataclysmic binaries. In all cases a high surface gravity and a high accretion rate are required to obtain short interflash periods.

The dependence of interflash period on various parameters may be qualitatively understood as follows. It turns out that pressure required for the ignition of nuclear fuel is roughly constant for a broad range of models. For example, it is about $10^{17.5}$ g cm^{-2} s^{-1} for degenerate dwarfs accreting hydrogen-rich matter. As a consequence of hydrostatic equilibrium the surface mass density may be calculated as the ratio of pressure to gravitational acceleration, $\Sigma = P/g$. It follows that less mass has to be accreted to produce a nuclear flash in a model with a higher gravity. Therefore, the interflash period should decrease with increasing gravity and with increasing accretion rate, just as it is seen in Figures 8 and 9. If the heat flux from the core is increased with all other parameters kept constant, then a smaller optical depth, i.e., less matter, is required to raise the temperature at the bottom of accreted layer to the point of nuclear ignition. Therefore, the interflash period should decrease with increasing heat flux from the core, just as shown in Figure 8.

It is interesting that almost all unstable models developed large-amplitude flashes, even if they were only marginally unstable with respect to small perturbations. I studied a few cases of a transition from models undergoing large-amplitude flashes to models that were stable by gradually changing the accretion rate. In all cases the transition was very abrupt: it took place within one flash cycle, and at the same value of accretion rate at which models with a steady-state nuclear burning became marginally stable against small perturbations. There was no gradual decline of the flash amplitude, just within one flash cycle it would decrease from a large value to zero.

There was only one region in the parameter space in which the full-scale flashes looked like slightly distorted sinusoidal oscillations with a modest amplitude. That was the region where the heat flux from the core was close to its maximum value for which models were still unstable, and where the length of the unstable branch of a linear series was very small. For example, a model with the parameters $\log g = 8.5$, $\log f_b = -0.77$, $\log \dot{a} = -0.65$, $X = 0.7$, $Z = 0.03$ is in such a region (cf. Fig. 6 or 7). These models were difficult to study with numerical integrations of the differential equations (15) because their full-scale flashes were only slightly nonlinear.

There are some aspects of shell flashes that are treated badly with the one-zone model. Here are some examples of those. The peak luminosity of flashes on

degenerate dwarfs comes very close to the Eddington limit, while it should approach a lower value following from the core mass-luminosity relation (Paczyński 1970). That is a consequence of adopting a plane-parallel geometry. In a detailed evolutionary model like that of Paczyński and Żytkow (1978) a lot of heat is carried by matter that has been processed by the nuclear burning shell and that merges with the stellar core. After some time this matter cools off, and the heat diffuses out and contributes to the surface luminosity. In the one-zone model the heat carried by matter into the core is lost from the energy balance. As a result the total amount of energy radiated from the surface during one full flash cycle is smaller than the total amount of heat released in nuclear burning during that cycle. The extent of convective mixing cannot be obtained with the one-zone model as it has no spatial resolution. At low accretion rates, electron thermal conductivity becomes important and makes a one-zone model unacceptable because the total opacity does not increase monotonically with the optical depth in the bulk of accreted matter. This effect becomes important in neutron stars accreting at less than 10^{-4} of the critical rate (in units used in this paper). Fortunately, electron conductivity was not important for our models of accreting white dwarfs, even at the lowest accretion rates studied, as those were still too high for electron degeneracy to become strong. It is obvious that even though the one-zone model may be very convenient and useful for many purposes, it is not the right one for detailed studies of nuclear shell flashes. Its main advantage is its simplicity, which makes it attractive for teaching and for pilot studies.

It is a pleasure to acknowledge that the report of an anonymous referee helped to improve and clarify many points of this paper. This project was partly supported by NSF grant AST 79-22012.

REFERENCES

Barranco, M., Buchler, J. R., and Livio, M. 1980, *Ap. J.*, **242**, 1226.
Ergma, E. V., and Tutukov, A. V. 1980, *Astr. Ap.*, **84**, 123.
Fujimoto, M. Y. 1982, *Ap. J.*, **257**, 767.
Fujimoto, M. Y., Hanawa, T., and Miyaji, S. 1981, *Ap. J.*, **247**, 267.
Gabriel, M., and Ledoux, P. 1967, *Ann. d'Ap.*, **30**, 975.
Gabriel, M., and Noels-Grotsch, A. 1968, *Ann. d'Ap.*, **31**, 167.
Gallagher, J. S., and Starrfield, S. 1978, *Ann. Rev. Astr. Ap.*, **16**, 171.
Joss, P. C. 1981, in *IAU Symposium 93, Fundamental Problems in the Theory of Stellar Evolution*, ed. D. Sugimoto, D. Q. Lamb, and D. N. Schramm (Dordrecht: Reidel), p. 207.
Lewin, W. G. H., and Joss, P. C. 1981, *Space Sci. Rev.*, **28**, 3.
Paczyński, B. 1970, *Acta Astr.*, **20**, 47.
———. 1972, *Acta Astr.*, **22**, 163.
Paczyński, B. 1980, in *Highlights of Astronomy*, Vol. **5** (Dordrecht: Reidel), p. 437.
Paczyński, B., and Rudak, B. 1980, *Astr. Ap.*, **82**, 349.
Paczyński, B., and Żytkow, A. N. 1978, *Ap. J.*, **222**, 604.
Papaloizou, J. C. B., Pringle, J. E., and MacDonald, J. 1982, *M.N.R.A.S.*, **198**, 215.
Schwarzschild, M., and Härm, R. 1965, *Ap. J.*, **142**, 855.
Sienkiewicz, R. 1980, *Astr. Ap.*, **85**, 295.
Sion, E. M., Acierno, M. J., and Tomczyk, S. 1979, *Ap. J.*, **230**, 832.
Sugimoto, D., and Miyaji, S. 1981, in *IAU Symposium 93, Fundamental Problems in the Theory of Stellar Evolution*, ed. D. Sugimoto, D. Q. Lamb, and D. N. Schramm (Dordrecht: Reidel), p. 191.

Note added in proof.—I have recently become aware of a paper "Thermal Relaxation Oscillations in a Two-Zone Model" by J. R. Buchler and J. Perdang (*Ap. J.*, **231**, 524 [1979]) which addresses the same subject as this paper.

BOHDAN PACZYŃSKI: Princeton University Observatory, Peyton Hall, Princeton, NJ 08544